Blocked edges on Eulerian maps and mobiles: application to spanning trees, hard particles and the Ising model

2007 J. Phys. A: Math. Theor. 40 7411

(http://iopscience.iop.org/1751-8121/40/27/002)

IOP PUBLISHING JOURNAL OF PHYSICS A: MATHEMATICAL AND THEORETICAL

J. Phys. A: Math. Theor. **40** (2007) 7411–7440 doi:10.1088/1751-8113/40/27/002

Blocked edges on Eulerian maps and mobiles: application to spanning trees, hard particles and the Ising model

J Bouttier, P Di Francesco and E Guitter

Service de Physique Théorique, CEA/DSM/SPhT, Unité de recherche associée au CNRS, CEA/Saclay, 91191 Gif sur Yvette Cedex, France

E-mail: bouttier@spht.saclay.cea.fr, philippe@spht.saclay.cea.fr and guitter@spht.saclay.cea.fr

Received 7 February 2007, in final form 15 May 2007
Published 20 June 2007
Online at stacks.iop.org/JPhysA/40/7411

Abstract

We introduce Eulerian maps with blocked edges as a general way to implement statistical matter models on random maps by a modification of intrinsic distances. We show how to code these dressed maps by means of mobiles, i.e. decorated trees with labelled vertices, leading to a closed system of recursion relations for their generating functions. We discuss particular solvable cases in detail, as well as various applications of our method to several statistical systems such as spanning trees on quadrangulations, mutually excluding particles on Eulerian triangulations or the Ising model on quadrangulations.

PACS numbers: 05.50.+q, 04.60.Nc, 61.50.Ks, 64.60.−i

(Some figures in this article are in colour only in the electronic version)

1. Introduction

Enumeration of maps, i.e. connected graphs embedded in a surface, is a fundamental issue that has drawn the attention of mathematicians and physicists all over the years ever since the seminal series of papers of Tutte on the subject [1]. In physical applications, the subject was extended so as to include *statistical models* defined on the maps, by equipping them with 'matter' configurations, say of particles, dimers, spins or trees. These dressed maps were introduced as discrete realizations of random surfaces in the general framework of two-dimensional quantum gravity (2DQG) [2] for which many results have been obtained so far (see [3] for a review). Several techniques have been used to address this problem of counting maps, with their possible matter decorations generally weighted by Boltzmann factors. Besides the original recursive decomposition technique of Tutte, mainly applied to maps without matter, the most powerful approach was undoubtedly that based on matrix integrals [4]. Many results obtained that way display a simplicity contrasting with the high sophistication of the method.

In particular, most planar enumeration results involve algebraic generating functions. This led combinatorists to look for alternative and more constructive approaches that could explain this simplicity [5, 6]. Quite recently, a general technique was developed that relies on bijections between planar maps with possible decorations and families of decorated trees [7]. The bijections are of two different types. A first class of bijections [7–9], well adapted to maps with prescribed vertex valences, consists of a cutting algorithm of the map into a *blossom tree* that carries the minimal information needed to recover the map. A second class of bijections [10, 11] is well adapted to the dual version of the former, namely maps with prescribed face valences. It makes use of the intrinsic geodesic distance on the map to code it by a so-called labelled mobile, i.e. a tree decorated by integer labels recording this distance in a way that allows one to reconstruct the original map. Both methods were used to enumerate families of bicoloured planar maps, or equivalently their dual Eulerian maps, *in the absence of matter*, all displaying the standard 'square-root singularity' characteristic of pure gravity (if we omit non-generic, non-physical multicritical points). Still, one may in some cases reinterpret the colour as a matter degree of freedom via suitable weightings. This gives access for instance to the solution of the Ising model on tetravalent maps [12], leading to a new singular behaviour of the generating function at the price of some analytic continuation to reach the transition point. Similarly, this allows us to treat the case of hard particles on arbitrary (non-bicoloured) maps, but with no new singular behaviour in this case [13].

In [14], it was found how to extend the bijection with blossom trees to the case of bicoloured maps equipped with interacting particles, allowing in particular to recover in a purely combinatorial way the crystallization transition of hard particles. Considering more involved particle exclusion rules leads to most of the possible universality classes of rational conformal theories (RCFT) with central charge $c < 1$ coupled to 2DQG [15].

The aim of this paper is to extend the mobile formalism to this same family of bicoloured (or dually Eulerian) maps with mutually excluding particles. As we shall see however, our method proves more general and applies to other classes of matter such as spanning trees or Ising spins, here without analytic continuation, thus providing a unified framework for all these models. More precisely, as already mentioned, the original mobile coding of Eulerian maps uses the geodesic distance from a given origin vertex on the map. A way to incorporate matter is precisely to modify this distance by introducing *blocked edges*, i.e. edges excluded from geodesic paths. All the matter systems above can indeed be reformulated in terms of configurations of blocked edges on Eulerian maps. The mobile construction is then easily modified so as to account for the presence of the blocked edges and this eventually leads to an efficient coding of the maps at hand in the form of labelled trees with marked edges. Using the tree structure, one can derive recursive equations for the corresponding generating functions, leading to a combinatorial solution of the original problems.

The paper is organized as follows. Section 2 is devoted to the general theory of map coding via mobiles. We first define precisely in section 2.1 the notion of Eulerian maps with blocked edges and show in section 2.2 how to code them by labelled mobiles that we characterize in detail. The procedure leading back from the mobile to the original map is described in section 2.3. In section 2.4, we further use the characterization of mobiles to obtain a system of recursive equations for their generating functions, also easily translated into map generating functions.

Sections 3 and 4 describe two large classes of applications. In section 3, a first series of direct applications consists of models where the blocked edges themselves form the matter degrees of freedom. Section 3.1 deals with the statistics of Eulerian maps with bi- and tetra-valent faces and with blocked edges, which can also be viewed as decorated quadrangulations whose unoriented edges can be blocked in both directions independently,

like maps with possible one-way roads and/or fully blocking roadworks. The simpler case of quadrangulations with fully blocked edges only is treated in section 3.2 where a detailed analysis of the critical singularities is presented. This allows in particular to solve the problem of quadrangulations with a spanning tree. In appendix A, we provide for both solutions a simple combinatorial interpretation in terms of maps with vertices of even valence and without matter. Appendix B deals with the case of maximally blocked Eulerian maps, i.e. maps with a maximal number of blocked edges but which remain connected in the sense that every vertex can still be reached via some path from the origin.

Section 4 is devoted to applications to maps with particles subject to exclusion rules. We first show in section 4.1 how to formulate these problems in terms of Eulerian maps with blocked edges by associating with any unconstrained configuration of particles on a map a set of configurations of blocked edges on the same map with possible negative weights, and whose total contribution vanishes as soon as the particle exclusion rule is violated. This allows for the derivation in section 4.2 of recursive relations for the generating functions of the models. Two particular examples are discussed: Eulerian triangulations with hard particles in section 4.3 and, in section 4.4, the Ising model on quadrangulations via a straightforward bijection with hard particles. We gather a few concluding remarks in section 5.

2. Coding maps with mobiles

Eulerian maps are planar embedded graphs (considered up to continuous deformation), which may be drawn in a single loop without lifting the pen. As each vertex is of even valence, the edges of these maps are naturally oriented, with incoming and outgoing edges alternating around each vertex. We may then imagine a walker moving along these oriented edges as on one-way streets throughout the map. We wish here to introduce the notion of Eulerian map with *blocked edges*, by which we simply mean that some of the edges of the map may be forbidden to the walker, like streets blocked by road works or so. The precise position of the blocked edges will be in general arbitrary up to one important restriction: we demand that every vertex of the map may be reached from a chosen origin vertex despite the blockings. As we shall see later, many statistical models on random maps may be described in terms of such Eulerian maps with blocked edges. This includes for instance spanning trees, hard particles, or even Ising spins.

2.1. Eulerian maps with blocked edges

Let us now come to more precise definitions of Eulerian maps with blocked edges. An Eulerian map is equivalently defined as a planar map whose faces are coloured in black and white so that no two adjacent faces be of the same colour. In other words, its dual map[1] is a bipartite planar map, namely a map whose vertices may be partitioned into two subsets such that no two vertices of the same subset are adjacent. The colouring of the faces of an Eulerian map induces a natural orientation of its edges by simply demanding for instance that this orientation be clockwise around black faces. Here we shall consider so-called pointed maps, i.e. maps with a distinguished vertex, hereafter referred to as the *origin*.

By map with blocked edges, we simply mean that we restrict the set of paths allowed on the map by deciding that some of the edges of the map are 'blocked', while paths are only allowed to pass through un-blocked edges and must respect the orientation on these

[1] Recall that the dual of a planar map is the planar map obtained by replacing each face by a vertex at its centre and each edge by a 'perpendicular' edge connecting the centres of the adjacent faces. The vertices of the original map become the faces of the dual map.

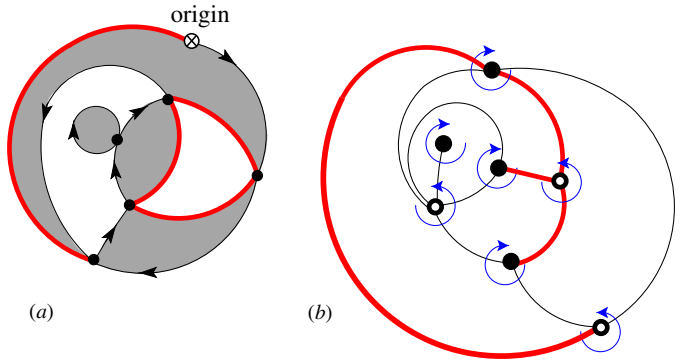

Figure 1. An example (*a*) of a pointed Eulerian map with blocked edges (thick lines). The blockings satisfy the global connectivity constraint that every vertex can be reached from the origin by a path consisting of non-blocked edges taken in their canonical orientation (indicated by an arrow). On the dual bipartite map (*b*), the duals of blocked edges necessarily form a forest, i.e. a graph without cycles and, moreover, are such that each face can be reached from the external face (dual to the origin) without crossing the forest edges and by going clockwise (resp. anticlockwise) around black (resp. white) vertices.

edges. As mentioned above, we furthermore impose a global *connectivity constraint* that each vertex be attainable from the origin by some allowed path (see figure 1(*a*) for an example). From this requirement, we immediately see that, on the dual bipartite map, the set of edges dual to blocked edges (also referred to as blocked edges for convenience) forms a forest, i.e. contains no cycle. This forest is however not arbitrary in general as it must be such that any face of the dual map can be reached from the origin face (dual of the origin vertex of the Eulerian map) without crossing blocked edges and by going clockwise (resp. anticlockwise) around black (resp. white) vertices (see figure 1(*b*)). The connectivity constraint is crucial for the construction below to be valid. In the following, we shall be led to introduce further restrictions on the blocked edge configurations, whose consequence on our construction will be transparent.

2.2. Well-labelled mobile construction

The connectivity constraint above allows us to assign to each vertex of the map its (finite) *distance* from the origin defined as the minimal number of steps of a path going from the origin to that vertex via un-blocked edges only and respecting the orientation. Such a path will be referred to as a *geodesic* path.

We can encode the configuration of the map and its blocked edges via a so-called well-labelled mobile as follows.

(1) We first label all vertices of the map by their distance from the origin.

(2) We then add a white (resp. black) vertex at the centre of each white (resp. black) face.

(3) We then consider each edge of the map and apply the following construction.

  (i) If the selected edge is a blocked edge, we draw its dual edge by connecting the black and white vertices at the centre of its adjacent faces and complete it with a *flag* on each side. We put on each flag the label of the closest vertex (see figure 2(i)). We finally *mark* this dual edge.

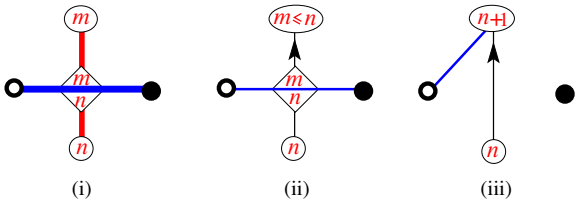

Figure 2. The rules for the construction of a well-labelled mobile (see text). A flagged edge can be marked (thick line) or not (thin line) according to whether the dual edge was blocked (i) or not (ii).

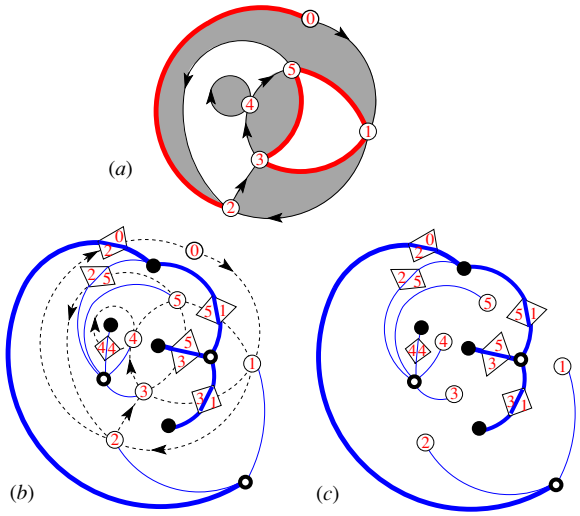

Figure 3. Construction of the well-labelled mobile associated with the Eulerian map with blocked edges (*a*) of figure 1. Applying the rules of figure 2 for each edge of the map (*b*) results in the desired mobile (*c*). On this mobile, flagged edges can be marked (thick lines) or not.

If the selected edge is not blocked, it points from a vertex at distance n from the origin to a vertex at distance m, with necessarily $m \leqslant n+1$.

(ii) If $m \leqslant n$, we repeat the above construction and draw the dual edge by connecting the black and white vertices at the centre of its adjacent faces and complete it with a flag on each side, with again the same label as that of the closest vertex (see figure 2(ii)). The dual edge is however un-marked in this case.

(iii) If $m = n+1$, we draw an edge from the white vertex at the centre of the adjacent white face to the vertex labelled $m = n+1$ (see figure 2(iii)).

The well-labelled mobile is simply defined as the graph obtained from the collection of all the black and white vertices, all the added marked (case (i)) and un-marked (case (ii)) flagged edges with their labelled flags, and all the added edges from white vertices (case (iii)) together with their labelled endpoints (see figure 3 for an example). For convenience, we shall refer to marked flagged edges, un-marked flagged edges and edges between white vertices and labelled vertices as edges of type (i), (ii) and (iii) respectively. Note that, by construction, all labels on labelled vertices are positive integers (since the origin vertex cannot be in the mobile), while

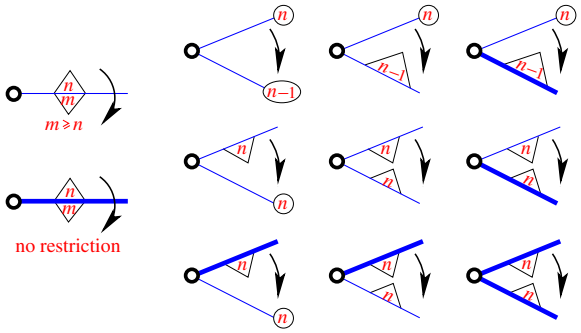

Figure 4. Constraints on the labels around a white vertex of a mobile (see text).

all labels on flags are non-negative integers. The above construction extends that of [11] that associates well-labelled mobiles with Eulerian maps without blocked edges by use of (ii) and (iii) only.

Let us now come to the characterization of the well-labelled mobiles obtained from this construction. The first and most important characterizing property of a well-labelled mobile is that it is a tree, i.e. a connected graph without cycles. The proof is similar to that of [11]. First we note that edges belonging to a geodesic path yield only un-marked edges of type (iii) in the mobile, as the distance increases by one at each step. This guarantees that geodesic paths on the map never cross the flagged edges of the mobile, and may cross the mobile only at its labelled vertices. We then assume by contradiction the existence of a cycle on the mobile, and call interior the region delimited by this cycle that does not contain the origin. We then consider the smallest label n among the labels of the (labelled) vertices on the cycle and the labels of the flags along the cycle that lie in the interior region. If n is attained for a labelled vertex on the cycle, we immediately deduce from the construction (iii) the existence of a vertex at distance $n-1$ from the origin in the interior. Any oriented geodesic path from the origin to that vertex must intersect the cycle at a labelled vertex with label strictly smaller than n. This is a contradiction. If n is not attained at a labelled vertex, but only at a flag, we deduce from the construction (i) or (ii) the existence of vertex at distance n from the origin in the interior; hence, a geodesic path to that vertex intersects the cycle at a labelled vertex with label $\leqslant n$. This is again a contradiction. We deduce that the mobile has no cycle, hence is a forest made of c connected components, where c is also the difference between its number of nodes and its number of edges. By construction, this number of edges is simply the number E of edges of the original map, while the number of nodes is equal to the number of faces F of the original map plus the number of labelled vertices. The latter is at most $V-1$ if we denote by V the total number of vertices of the original map, as the origin cannot belong to the mobile (it remains isolated by construction hence is removed). As $F+V-E=2$ from the Euler relation for a planar map, we deduce that $c \leqslant F+(V-1)-E=1$, hence necessarily $c=1$. The mobile is thus a tree that moreover contains all the vertices of the original map but the origin.

The second characterizing property of well-labelled mobiles concerns the environment of white and black vertices, i.e. the configuration of labels around them. Recall that, by *corner* at a vertex is meant any sector delimited by two consecutive incident edges around that vertex. In the case of a white vertex, we first note that, by construction, the number of incident edges

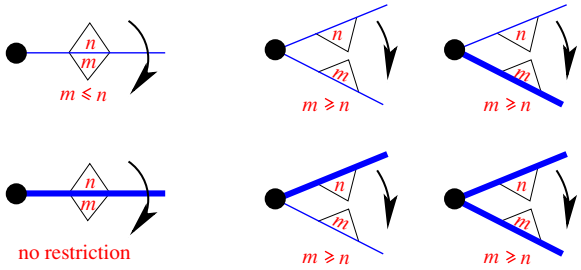

Figure 5. Constraints on the labels around a black vertex of a mobile (see text).

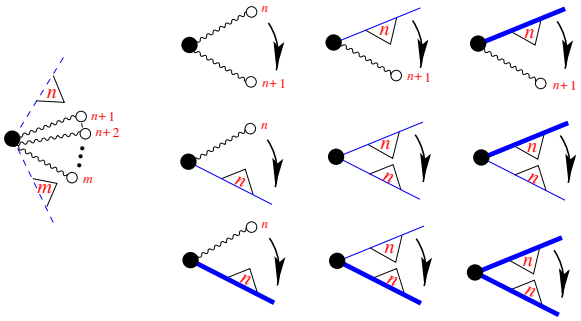

Figure 6. An alternative representation using spurious dangling edges of the constraints of figure 5 for the evolution of labels at a corner around a black vertex.

is nothing but the valence of the associated white face on the original map. We have the following rules for the cyclic evolution of the labels around each white vertex (see figure 4):

- at the *crossing* of each un-marked flagged edge, the value of the flag must increase weakly clockwise. There is *no such restriction for marked flagged edges*;
- going through each *corner* clockwise around a white vertex, the label decreases by one if the first edge of the corner is of type (iii), and remains constant if the first edge is of type (i) or (ii).

As for black vertices, their incident edges are of type (i) and (ii) only and we have the following rules for the cyclic evolution of the labels around each black vertex (see figure 5):

- at the crossing of each un-marked flagged edge, the value of the flag must decrease weakly clockwise. There is no such restriction for marked flagged edges;
- going through each corner clockwise around a black vertex, the label increases weakly.

Note that the first (crossing) rules for white and black vertices are actually redundant with each other, but we mention both of them to emphasize the symmetry. Moreover, as displayed in figure 6, the second (corner) rule for black vertices can be made similar to that of white vertices by dressing each corner around a black vertex with first label n and second label $m \geqslant n$ clockwise by $m - n$ spurious dangling (wiggled) edges attached to spurious vertices labelled $n + 1, n + 2, \ldots, m$. With this dressing, the black corner rule becomes

- going through each corner clockwise around a black vertex, the label increases by one if the last edge of the corner is a dangling edge and remains constant if the last edge is of type (i) or (ii).

In this latter formulation, the total number of edges around a black vertex, including the spurious ones, is nothing but the valence of the associated black face on the original map.

The above properties for the evolution of labels, together with the fact that these labels are positive integers on vertices and non-negative integers on flags, with at least one vertex labelled 1 or one flag labelled 0, form a complete characterization of the well-labelled mobiles. In the following, we will be led to relax the above constraints on labels. Mobiles for which we relax the constraint of existence of a label 1 or 0 but keep the positivity constraint will be referred to as *positive mobiles*. Finally, mobiles for which we relax both constraints will simply be referred to as *unrestricted mobiles*.

2.3. Inverse construction

The well-labelled mobiles constructed above form compact encodings of the associated Eulerian maps with blocked edges. Indeed, to recover the original map and its blocked edges from the corresponding mobile, we simply apply the construction of [11] as follows. First, by *labelled corner* we simply mean a corner at a labelled vertex of the mobile, with the corresponding label value. We then move clockwise *around the mobile* and record the cyclic sequence of successive labels encountered at flags and/or labelled corners (spurious edges and vertices displayed in figure 6 are not considered). The passage from a label to the next is always via a white or a black vertex, hence, from the rules obeyed by labels around those vertices, we immediately deduce that the sequence of labels decreases by one after each labelled corner and increases weakly after each flag (in particular, it remains constant when passing along a white vertex). Otherwise stated, the sequence of labels around the mobile has the 'ratchet' property that it can have arbitrary increasing steps but decreasing steps of *at most* 1 which take place just after labelled corners.

This property immediately ensures the existence of *successors* defined as follows: the successor of a labelled corner with label $n > 1$ is the first labelled corner encountered clockwise with label $n - 1$. Similarly, the successor of a flag with label $n > 0$ is the first labelled corner encountered clockwise with label n. Note that the ratchet property of the label sequence also guarantees that if a corner or flag l' lies between a corner or flag l and its successor $s(l)$, the successor $s(l')$ is necessarily attained at or before $s(l)$. We may therefore connect each labelled corner with label $n > 1$ and each flag with label $n > 0$ to its successor by a new edge, called a *chord*, in such a way that all these chords do not cross, while all corners labelled 1 and all flags labelled 0 remain adjacent to the exterior face. We finally add an extra origin vertex inside the exterior face and connect all corners labelled 1 and all flags labelled 0 to that vertex by non-crossing chords. The original Eulerian map is made of the origin, the labelled vertices and the chords. Note that some chords (those starting from flags) have to be glued at the level of the double flags so as to form the desired edges between the (origin or labelled) vertices of the map (see figure 7 for an example). Any edge of the Eulerian map is of one of the following three types (see figure 7).

(i) Either it is obtained by gluing two chords at the level of the double flag of a marked edge. We then make it a blocked edge.
(ii) Or it is obtained by gluing two chords at the level of the double flag of an un-marked edge. This edge is then left un-blocked and we decide to orient it so that the black endpoint of the flagged edge lies on its right.
(iii) Or it is obtained from a single chord connecting a labelled vertex to its successor. This edge is then left un-blocked and we decide to orient it backwards from the successor.

The proof that the above construction and that of the previous section are inverse of one another is similar to that of [11] in the absence of blocked edges and will not be reproduced

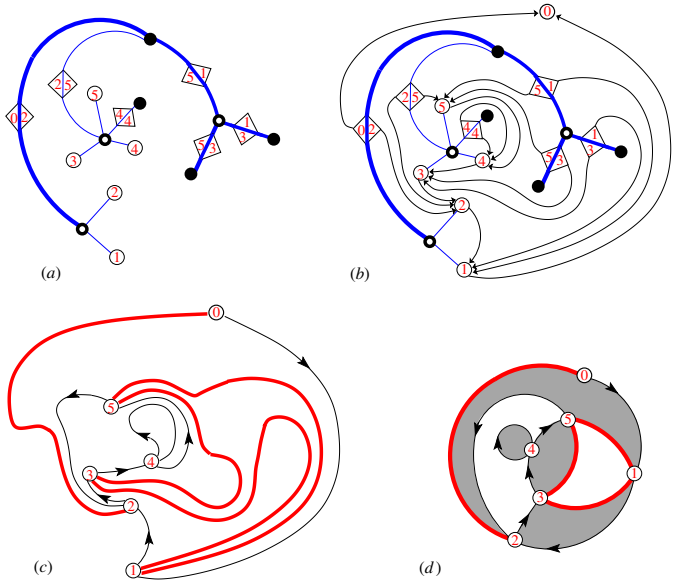

Figure 7. Inverse construction: starting from a well-labelled mobile (*a*), each labelled corner or flag is connected to its successor (*b*). The graph formed by these chords (*c*) is the desired Eulerian map (*d*), where the blocked edges are obtained from the chords originating from marked flagged edges.

here. The orientation of the edges simply reproduces that induced by the black and white faces on the Eulerian map. Finally, the labels on the vertices simply record the distance of these vertices form the origin by oriented paths avoiding blocked edges. Indeed, form our choice of orientation above, the sequence of labels along any oriented path from the origin on the map either decreases weakly (case (ii) above) or increases by one (case (iii) above) at each step. The label of a vertex is therefore necessarily smaller than its distance from the origin. In other words, the distance from the origin to a vertex is larger or equal to its label, and it must be exactly equal as the sequence of consecutive successors of that vertex provides, when considered backwards, an oriented path from the origin to that vertex whose length is exactly equal to its label.

2.4. Generating series

The main interest of the above coding by mobiles concerns the *enumeration* of families of Eulerian maps with blocked edges. Indeed, such enumeration simply amounts to counting appropriate mobiles and the underlying tree structure of these mobiles translates into simple recursive equations for the associated generating functions.

In the following, we shall consider only mobiles with at least one labelled vertex. In other words, we exclude the degenerate case of mobiles made only of flagged edges, necessarily all with equal labels. Going back to maps, this amounts to excluding the quite trivial maps made of a single vertex only, connected by a configuration of nested 'petals'. The enumeration of mobiles is then made easier by considering *rooted* mobiles, i.e. mobiles with a distinguished corner around a labelled vertex. We may then view the mobile as hanging from an extra root edge added in this corner.

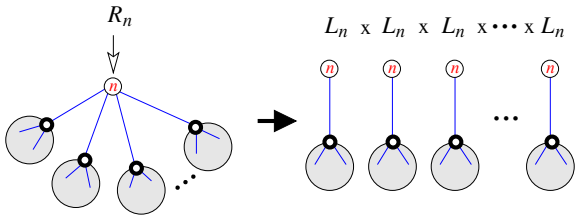

Figure 8. Recursive decomposition of a mobile rooted at a labelled corner. When the root vertex has valence k, the decomposition yields k mobiles rooted at a univalent labelled vertex. In terms of generating function, this translates into equation (2.1).

Let us now consider the quite general problem of enumerating maps with *prescribed face valences* and with a fixed number of blocked edges. At this stage, we make for simplicity no restriction on the configuration of blocked edges around a face other than the global connectivity constraint. Some extra restrictions will be introduced in some applications below, whose incorporation will lead to straightforward and harmless modifications. As usual, it is simpler to work within grand canonical ensembles of maps in which the numbers of faces of given valences may vary and are controlled by weight factors. More precisely, we consider the set of maps with faces of arbitrary valences up to some upper bound p, counted with weight g_k per k-valent white face, $\tilde{g}_k$ per k-valent black one ($k = 1, 2, \ldots, p$). We also let the number of blocked edges vary, with a weight y per blocked edge. This amounts to consider mobiles with white and black vertices of valence $k \leqslant p$ (including the spurious dangling edges for black vertices), weighted respectively by g_k and $\tilde{g}_k$, and with an arbitrary number of marked edges weighted by y.

We denote by R_n the generating function of such weighted mobiles rooted at a corner labelled n. At this stage, we need not specify whether the labels obey positivity conditions (case of positive mobiles) or not (case of unrestricted mobiles). Indeed, the following reasoning holds in both cases, the difference coming only from boundary conditions that we shall discuss later. We shall not consider the case of well-labelled mobile (rooted at a corner labelled n) as their generating function G_n is directly expressed in terms of that for positive mobiles via $G_n = R_n - R_{n-1}$.

Let us derive the set of recursion relations for R_n inherited from the mobile structure. We have the first relation

$$R_n = \sum_{k=0}^{\infty} (L_n)^k = \frac{1}{1 - L_n}, \tag{2.1}$$

where L_n is the generating function of mobiles rooted at a *univalent* vertex labelled n. This is readily seen by decomposing the root vertex according to its arbitrary valence k (see figure 8).

The generating function L_n is then obtained by inspecting the environment of the white vertex attached to the univalent root vertex. Its descendent subtrees come into three species (see figure 9):

(i) sub-mobiles rooted at a corner around a labelled vertex, with generating function R_i if the root label is i,

(ii) sub-mobiles rooted at some un-marked flagged edge incident to a black vertex, with generating function $B_{i,j}$ if i (resp. j) is the label on the right (resp. left), viewed with the white vertex on top,

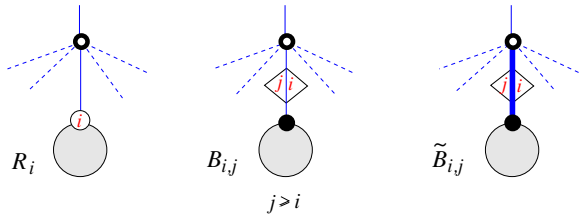

Figure 9. The three possible types of descending subtrees at a white vertex of a mobile according to the type of their root edge, together with the associated generating functions.

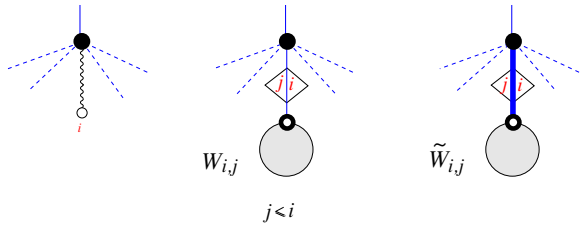

Figure 10. The three possible types of descending subtrees at a black vertex of a mobile according to the type of their root edge, together with the associated generating functions. It proves convenient to use the representation of figure 6 of mobiles with spurious dangling edges (with a trivial generating function 1) which emphasizes the similarity between black and white vertices.

(iii) sub-mobiles rooted at some marked flagged edge incident to a black vertex, with generating function $\tilde{B}_{i,j}$ if again i (resp. j) is the label on the right (resp. left).

To follow the evolution of labels clockwise around the inspected white vertex, we introduce a formal (transfer) operator $\mathbf{Q}_\circ$ acting on basis vectors $|i\rangle$ indexed by the encountered labels. The action of this operator reads

$$\mathbf{Q}_\circ|i\rangle = R_i|i-1\rangle + \sum_{j\geqslant i} B_{i,j}|j\rangle + \sum_j \tilde{B}_{i,j}|j\rangle, \tag{2.2}$$

where the ranges of summation incorporate the white crossing rules (obeyed by labels at the crossing of flagged edges) displayed in figure 4. Returning to the computation of L_n, we note that, as the first label encountered clockwise is $n-1$, the succession of labels around the white vertex must lead from $n-1$ back to n in $k-1$ steps if the white vertex is k-valent. This leads to

$$L_n = \sum_k g_k \langle n|\mathbf{Q}_\circ^{k-1}|n-1\rangle, \tag{2.3}$$

where $\langle i|$ denotes a vector of the dual basis defined by $\langle i|j\rangle = \delta_{i,j}$.

Likewise, inspecting the environment of a black vertex incident to a flagged root edge, we get

$$B_{i,j} = \sum_k \tilde{g}_k \langle j|\mathbf{Q}_\bullet^{k-1}|i\rangle, \qquad j \geqslant i \tag{2.4}$$

and

$$\tilde{B}_{i,j} = y \sum_k \tilde{g}_k \langle j|\mathbf{Q}_\bullet^{k-1}|i\rangle, \tag{2.5}$$

where the transfer operator $\mathbf{Q}_\bullet$ around a black vertex now reads

$$\mathbf{Q}_\bullet|i\rangle = |i+1\rangle + \sum_{j\leqslant i} W_{i,j}|j\rangle + \sum_j \tilde{W}_{i,j}|j\rangle. \tag{2.6}$$

Here the three terms account for the three species of sub-mobiles one may encounter around a black vertex (see figure 10):

(i) dangling ends with weight 1,
(ii) sub-mobiles rooted at some un-marked flagged edge incident to a white vertex, with generating function $W_{i,j}$ if i (resp. j) is the label on the right (resp. left), viewed with the black vertex on top,
(iii) sub-mobiles rooted at some marked flagged edge incident to a white vertex, with generating function $\tilde{W}_{i,j}$ if again i (resp. j) is the label on the right (resp. left).

The ranges of summation in equation (2.6) now incorporate the black crossing rules (obeyed by labels at the crossing of flagged edges) displayed in figure 5. The generating functions $W_{i,j}$ and $\tilde{W}_{i,j}$ are finally obtained from

$$W_{i,j} = \sum_k g_k \langle j|\mathbf{Q}_\circ^{k-1}|i\rangle, \qquad j \leqslant i \tag{2.7}$$

and

$$\tilde{W}_{i,j} = y \sum_k g_k \langle j|\mathbf{Q}_\circ^{k-1}|i\rangle. \tag{2.8}$$

Let us now discuss the distinction between positive and unrestricted mobiles. In the case of positive mobiles, equations (2.1)–(2.8) above are only valid for the allowed range of labels, i.e. $n > 0$ for R_n and L_n and $i, j \geqslant 0$ for $B_{i,j}$, $\tilde{B}_{i,j}$, $W_{i,j}$ and $\tilde{W}_{i,j}$. Moreover, in equations (2.2) and (2.6), we must implicitly assume that $R_i = 0$ for $i \leqslant 0$ and $B_{i,j} = \tilde{B}_{i,j} = 0$ as well as $W_{i,j} = \tilde{W}_{i,j} = 0$ if $i < 0$ or $j < 0$. With these conditions, the set of equations (2.1)–(2.8) determine completely all generating functions as formal power series of the g_k's and the $\tilde{g}_k$'s.

The case of unrestricted labels is much simpler as (2.1)–(2.8) are valid for all values of the indices and moreover, enjoy a manifest translation invariance property. More precisely, we may write

$$\begin{array}{llll} R \equiv R_n & B_\ell \equiv B_{n,n+\ell} & \ell \geqslant 0 & \tilde{B}_\ell \equiv \tilde{B}_{n,n+\ell} \\ & W_\ell \equiv W_{n,n+\ell} & \ell \leqslant 0 & \tilde{W}_\ell \equiv \tilde{W}_{n,n+\ell} \end{array} \tag{2.9}$$

as all the above quantities on the right-hand side are independent of n.

Going back to maps, one can easily check that R is the generating function for Eulerian maps with blocked edges, with an origin vertex and with a *distinguished edge* which is not blocked and moreover points from a vertex at distance m from the origin to one at distance $m+1$, for some m. Indeed, we have clearly a bijection between the set of well-labelled mobiles rooted at a corner with *arbitrary* label, and the set of unrestricted mobiles rooted at a corner with *prescribed* label (say 0), whose generating function is R. The bijection simply consists in shifting all labels of the well-labelled mobile by a constant value, such that the root label becomes 0. Finally, the corners labelled $m+1$ on a well-labelled mobile are in correspondence with non-blocked edges of type $m \to m+1$ on the corresponding map.

One may as well distinguish an edge on the map which is not blocked, but now points from a label at distance m from the origin to a label at distance $m-\ell$ ($\ell \geqslant 0$) for some arbitrary m. The corresponding generating function is easily seen to be $B_\ell W_{-\ell}$. Finally, one may also distinguish an edge which is blocked and connects a vertex at distance m from the origin to

a label at distance $m-\ell$ for some arbitrary m. The corresponding generating function reads $(1/y)(\tilde{B}_\ell \tilde{W}_{-\ell} + \tilde{B}_{-\ell}\tilde{W}_\ell)$ for $\ell \neq 0$ and $(1/y)\tilde{B}_0\tilde{W}_0$ for $\ell = 0$. To summarize, the generating function of pointed Eulerian maps with blocked edges and with a *distinguished non-blocked edge* is

$$R + \sum_{\ell \geqslant 0} B_\ell W_{-\ell} \tag{2.10}$$

while that of pointed Eulerian maps with blocked edges and with a *distinguished blocked edge* is

$$\frac{1}{y}\sum_{\ell} \tilde{B}_\ell \tilde{W}_{-\ell}. \tag{2.11}$$

The functions $R, B_\ell, W_\ell, \tilde{B}_\ell$ and $\tilde{W}_\ell$ are the translation invariant solutions of equations (2.1)–(2.8), which can be rewritten in a slightly more compact form by introducing a formal variable z and defining the Laurent series $Q_\circ(z)$ and $Q_\bullet(z)$ via

$$\begin{aligned} Q_\circ(z) &= \frac{R}{z} + \sum_{\ell \geqslant 0} B_\ell z^\ell + \sum_{\ell} \tilde{B}_\ell z^\ell \\ Q_\bullet(z) &= z + \sum_{\ell \leqslant 0} W_\ell z^\ell + \sum_{\ell} \tilde{W}_\ell z^\ell \end{aligned} \tag{2.12}$$

that are translation invariant versions of equations (2.2) and (2.6). The recursive equations read

$$\begin{aligned} R &= \frac{1}{1-L}, \qquad & L &= \sum_k g_k Q_\circ(z)^{k-1}|_{z^1} \\ B_\ell &= \sum_k \tilde{g}_k Q_\bullet(z)^{k-1}|_{z^\ell}, \qquad & \ell &\geqslant 0 \\ \tilde{B}_\ell &= y\sum_k \tilde{g}_k Q_\bullet(z)^{k-1}|_{z^\ell} & & \\ W_\ell &= \sum_k g_k Q_\circ(z)^{k-1}|_{z^\ell}, \qquad & \ell &\leqslant 0 \\ \tilde{W}_\ell &= y\sum_k g_k Q_\circ(z)^{k-1}|_{z^\ell} & & \end{aligned} \tag{2.13}$$

where $|_{z^\ell}$ stands for the extraction of the coefficient of z^ℓ in the corresponding Laurent series.

Eliminating L, all B's and W's, we arrive at the closed system of equations

$$\boxed{\begin{aligned} Q_\circ(z) &= \frac{R}{z} + \sum_k \tilde{g}_k \left[Q_\bullet^{k-1}(z)\right]_+ + y\sum_k \tilde{g}_k Q_\bullet^{k-1}(z) \\ Q_\bullet(z) &= z + \sum_k g_k \left[Q_\circ^{k-1}(z)\right]_- + y\sum_k g_k Q_\circ^{k-1}(z) \\ R &= 1 + \sum_k g_k \left[\frac{Q_\circ^{k-1}(z)}{z}\right]_0 R, \end{aligned}} \tag{2.14}$$

where the notations $[\cdot]_+$, $[\cdot]_-$ and $[\cdot]_0$ stand respectively for the extraction of the non-negative power part, the non-positive power part, and the constant term in the Laurent series. In practice, this system may be solved in two steps: the first two lines determine all coefficients of the Laurent series as functions of R and formal power series of the g's and $\tilde{g}$'s. Substituting these in the third line yields a self-consistent equation for R, which itself is solved order by order in the g's and $\tilde{g}$'s.

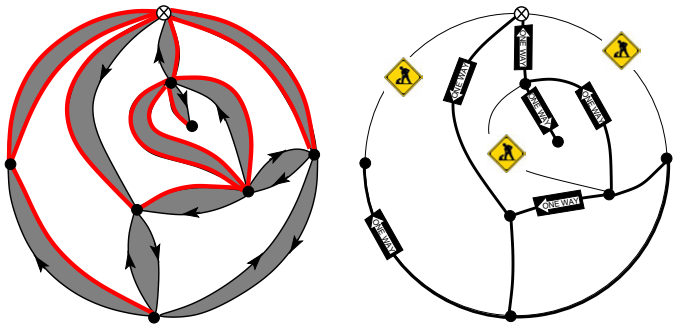

Figure 11. An example of pointed Eulerian map (left) with blocked edges (thick lines) satisfying the global connectivity constraint, where all black faces are bivalent and all white faces tetravalent. Each black face can be squeezed into an edge, resulting in a quadrangulation (right) whose edges can be either non-blocked (thick lines), blocked in one direction only (thick lines with one-way signs) or blocked in both directions (thin lines with roadwork signs).

When $y = 0$ we recover the usual equations for Eulerian maps (without blocked edges), as obtained from the mobile construction of [11] or by the so-called orthogonal polynomial solution of the two-matrix model. It is interesting to note that the restriction of Laurent series to their positive or negative parts simply reflects the constraints on flag labels for un-marked edges (crossing rules). For marked edges (corresponding to the y term) there is no such restriction.

Finally, we have the *duality* property that, whenever $g_k = \tilde{g}_k$ for all k, $Q_\circ(z)$ is equal to $Q_\bullet\left(\frac{R}{z}\right)$, while R can be alternatively recovered via

$$R = 1 + \sum_k g_k [Q_\bullet(z)^{k-1} z]_0. \tag{2.15}$$

3. Direct applications

In this section, we show for illustration how to use the above formalism to study the statistics of blocked edges in a number of simple cases in which the blocked edges themselves form the matter degrees of freedom on the maps.

3.1. Blocked edges on quadrangulations viewed as Eulerian maps

As a first direct application of the results of section 2, let us consider the simple case of quadrangulations viewed as Eulerian maps as follows: consider Eulerian maps where all white faces are tetravalent and all black faces are bivalent. We may squeeze all the black faces into single edges, which results in a (non necessarily Eulerian) map with tetravalent faces only, i.e. a quadrangulation. After this transformation, every edge replaces two edges of the original map, with opposite orientations. Hence, in the absence of blockings, each edge of the quadrangulation can now be taken in both directions. The introduction of blockings now corresponds to forbidding either one direction (one way road) or both, keeping the global connectivity constraint that every vertex be reachable from the origin of the map (see figure 11 for an example). Taking equation (2.14) with $g_k = g\delta_{k,4}$ and $\tilde{g}_k = \delta_{k,2}$ (as there are

exactly twice as many black bivalent faces as white tetravalent ones, we need not introduce an extra weight factor for the black faces), we get the system:

$$\begin{aligned} Q_\circ(z) &= \frac{R}{z} + [Q_\bullet(z)]_+ + yQ_\bullet(z) \\ Q_\bullet(z) &= z + g\left[Q_\circ^3(z)\right]_- + gyQ_\circ^3(z) \\ R &= 1 + g\left[\frac{Q_\circ^3(z)}{z}\right]_0 R. \end{aligned} \tag{3.1}$$

First we note that, by parity, both $Q_\circ(z)$ and $Q_\bullet(z)$ contain only odd powers of z. From the second line, we then immediately deduce that

$$[Q_\bullet(z)]_+ = z + gy\left[Q_\circ^3(z)\right]_+ \tag{3.2}$$

and, upon substituting in the first line

$$Q_\circ(z) = \frac{R}{z} + (1+y)z + gy(1+y)Q_\circ(z)^3. \tag{3.3}$$

Upon setting $x = gy(1+y)(R/z+(1+y)z)^2$ and $Q_\circ(z) = (R/z+(1+y)z)q(x)$, this equation becomes

$$q(x) = 1 + xq(x)^3 \tag{3.4}$$

whose formal solution is

$$q(x) = \sum_{n\geqslant 0} \frac{(3n)!}{n!(2n+1)!}x^n. \tag{3.5}$$

Writing the last line of equation (3.1) as

$$\begin{aligned} R &= 1 + g\left[\frac{1}{gy(1+y)}\left(Q_\circ(z) - \frac{R}{z} - (1+y)z\right)\frac{1}{z}\right]_0 R \\ &= 1 + \sum_{n\geqslant 1} \frac{(3n)!}{n!(2n+1)!} g^n\,(y(1+y))^{n-1}\left[\left(\frac{R}{z} + (1+y)z\right)^{2n+1}\frac{1}{z}\right]_0 R, \end{aligned} \tag{3.6}$$

we end up with a single equation for the generating function R:

$$R = 1 + \sum_{n\geqslant 1} \frac{(3n)!}{n!n!(n+1)!} g^n y^{n-1}(1+y)^{2n} R^{n+1}. \tag{3.7}$$

Rather than directly analysing this formula, we will derive and study in the next section a very similar and slightly simpler formula (see equation (3.10)). Their connection is discussed in appendix A.

3.2. Blocked edges on quadrangulations and spanning trees on the dual

As there is no canonical orientation of the edges in quadrangulations, a more natural definition of blocked edges consists in either allowing for *both directions* on a given edge or forbidding both simultaneously. In the Eulerian map equivalent formulation of previous section, this simply means that blockings always take place for both directions simultaneously. In this case, for a fixed map, the configurations of blocked edges satisfying the global connectivity constraint turn out to be independent of the choice of the origin. Rephrased in the dual language, this constraint simply amounts to demand that the duals of blocked edges make no cycles, i.e. form a forest (see figure 12 for an example) with no further restriction. The

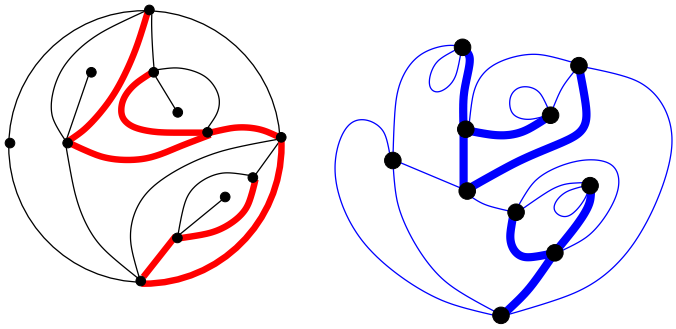

Figure 12. A quadrangulation (left) with edges (thick lines) blocked in both directions, and satisfying the global connectivity constraint (irrespectively of the choice of the origin vertex). On the dual tetravalent map (right), duals of blocked edges (thick lines) form a forest.

problem therefore amounts to enumerating *forests on planar maps* with tetravalent vertices, with a weight g per vertex and, say y per edge of tree in the forest.

Imposing that both direction be blocked simultaneously is achieved in the mobile language by requiring that every (bivalent) black vertex on the mobile has either 0 or 2 incident marked edges. This constraint results in a slight modification of equation (3.1), now replaced by

$$\begin{aligned} Q_\circ(z) &= \frac{R}{z} + [\bar{Q}_\bullet(z)]_+ + y\tilde{Q}_\bullet(z) \qquad & \bar{Q}_\bullet(z) &= z + g\left[Q_\circ^3(z)\right]_- \\ \tilde{Q}_\bullet(z) &= gQ_\circ^3(z) & R &= 1 + g\left[\frac{Q_\circ^3(z)}{z}\right]_0 R, \end{aligned} \tag{3.8}$$

which amounts to a splitting of the operator $Q_\bullet(z)$ of equation (3.1) into $\bar{Q}_\bullet(z)$ and $\tilde{Q}_\bullet(z)$ respectively corresponding to sub-mobiles with an un-marked and a marked root edge. The first three equations now reduce to

$$Q_\circ(z) = \frac{R}{z} + z + gyQ_\circ(z)^3 \tag{3.9}$$

from which we deduce the equivalent of equation (3.7) for the generating function R:

$$R = 1 + \sum_{n\geqslant 1} \frac{(3n)!}{n!n!(n+1)!} g^n y^{n-1} R^{n+1}. \tag{3.10}$$

For instance, the first few terms in the expansion of R as power series of g read

$$\begin{aligned} R = 1 &+ 3g + 6g^2(3+5y) + 15g^3(9+30y+28y^2) + 18g^4(63+315y \\ &+ 570y^2 + 385y^3) + 126g^5(81+540y+1440y^2+1855y^3+1001y^4) \\ &+ 36g^6(2673 + 22\,275y + 78\,300y^2 + 146\,970y^3 + 149\,884y^4 + 68\,068y^5) + \mathcal{O}(g^7), \end{aligned} \tag{3.11}$$

from which we read off the generating functions for forests on tetravalent maps (with distinguished face and unoccupied edge) with up to six vertices. In appendix A, we show how to reinterpret equation (3.10) in the language of even-valent maps without matter. Note that equation (3.10) is equivalent to equation (3.7) upon substituting $g \to g(1+y)^2$. The origin of this extra factor is also explained combinatorially in appendix A.

Let us now investigate the analytical behaviour of R as a function of g for a fixed finite positive value of y (note that each term of the series expansion of R in powers of g is a polynomial in y). Introducing the function

$$F(u) \equiv \sum_{n\geqslant 1} \frac{(3n)!}{n!n!(n+1)!} u^n, \tag{3.12}$$

we can rewrite equation (3.10) in a parametric form as

$$g = \frac{u(y-F(u))}{y^2} \qquad R = \frac{y}{y-F(u)}, \tag{3.13}$$

where we have introduced for convenience a parameter $u = gyR$. In this parametrization, u must lie between 0 and $1/27$, which is the radius of convergence of $F(u)$. However, the first equation determines implicitly u in terms of g only in a range in which $\mathrm{d}g/\mathrm{d}u$ does not vanish, namely $u \in [0, u^\star)$ where $u^\star$ is the smallest positive solution of $\mathrm{d}g/\mathrm{d}u(u^\star) = 0$. This last condition may be rewritten as

$$y = F(u^\star) + u^\star F'(u^\star) \tag{3.14}$$

which has a unique solution $0 < u^\star < 1/27$ for any finite positive value of y since the function $F(u) + uF'(u)$ strictly increases and maps $[0, 1/27)$ to $[0, +\infty)$. This implies that $u(g)$ has a finite radius of convergence $g^\star = u^\star(y - F(u^\star))/y^2$. Note that $\mathrm{d}^2g/\mathrm{d}u^2(u^\star) < 0$ which implies that the singularity of $u(g)$ is of the form $(u^\star - u(g)) \sim (g^\star - g)^{1/2}$. Finally, we easily see that the function $R(u)$ in (3.13) is regular in the range $[0, u^\star]$ (as $F(u) \leqslant F(u^\star) < y$ in this range) and $\mathrm{d}R/\mathrm{d}u(u^\star) > 0$. Hence $R(g)$ has the same radius of convergence $g^\star$ and the same square root singularity. This corresponds to a critical exponent $\gamma = -1/2$ (defined by $R(g^\star) - R(g) \sim (g^\star - g)^{-\gamma}$) characteristic of the universality class of so-called pure gravity, which is also found for quadrangulations without blocked edges.

Finally, a different singular behaviour is obtained by taking the $y \to \infty$ limit in equation (3.10), keeping $\alpha = gy$ fixed. In this limit, we readily see that $R = 1 + (1/y)F(\alpha) + \mathcal{O}(1/y^2)$ where $F(\alpha)$ can now be interpreted as the generating function of maps with tetravalent vertices and equipped with a *spanning tree*, i.e. a single connected tree passing via all the vertices of the map, and with a weight α per vertex. The map has as before a distinguished face (origin face) and a distinguished unblocked edges separating two faces at distance m and $m+1$ from the origin. We simply interpret the coefficient of α^n in $F(\alpha)$ as

$$\frac{(3n)!}{n!n!(n+1)!} = \frac{(3n)!}{n!(2n+1)!} \times \frac{(2n+2)!}{(n+1)!(n+2)!} \times (n+2) \times \frac{1}{2} \tag{3.15}$$

expressing, as displayed in figure 13, that our tetravalent map with a spanning tree is made of a rooted ternary tree with n inner vertices and $2n+2$ leaves (first factor), completed with a system of $n+1$ arches connecting these leaves (second factor) and forming the unvisited edges, with a choice of one among $n+2$ faces (third factor). The last factor $1/2$ is because the rooting of the ternary tree amounts to distinguish an *oriented* unvisited edge (that emerging from the root) while, in F, we distinguish only an un-oriented edge (here all edges are of type $m \to m+1$, irrespectively of the choice of origin). For $\alpha \to \alpha^\star \equiv 1/27$, we now have the singular behaviour $F(\alpha^\star) - F(\alpha) \sim (\alpha^\star - \alpha)\mathrm{Log}(\alpha^\star - \alpha)$, hence a critical exponent $\gamma = -1$. The same exponent was obtained in [16] for a slightly different model.

The above analysis applies straightforwardly to the case of section 3.1 by substituting $g \to g(1+y)^2$. Among other possible direct applications of equation (2.14), one may also consider the case of arbitrary Eulerian maps with a *maximal number of blocked edges*. This case is discussed in detail in appendix B.

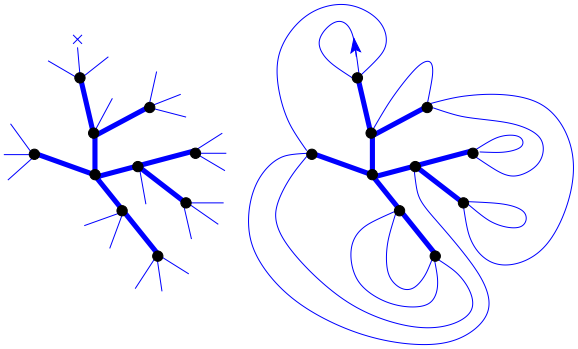

Figure 13. A rooted ternary tree (left). Upon matching leaves by pairs via a set of non-crossing arches, we obtain a tetravalent map endowed with a spanning tree, and with a distinguished oriented edge.

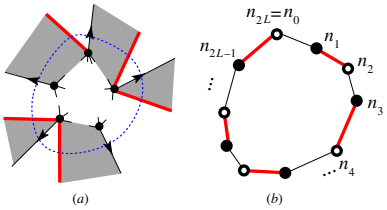

Figure 14. A piece of map (a) with blocked edges and with some maximal domain (inside the dashed line) which is not attainable from the origin of the map, supposed to lie outside of the figure. All potentially incoming edges are blocked so that no path can enter the domain. In the dual representation (b), the boundary of the domain is a loop of length $2L$ of alternating black and white vertices, each carrying a number n_i of particles, $i = 0, \ldots, 2L-1$ (and with $n_{2L} \equiv n_0$) and with every other edge blocked. We have $n_{2i-1} + n_{2i} \geqslant p+1$ for $i = 1, \ldots, L$; hence, there exists some $i_0 \in \{0, \ldots, L-1\}$ for which $n_{2i_0} + n_{2i_0+1} \geqslant p+1$. The corresponding edge may be freely blocked or not, thus contributing a weight $1 + y = 0$.

4. Applications to maps with hard particles

4.1. Particles with exclusion rules on maps

Besides the direct applications already mentioned, the main interest of Eulerian maps with blocked edges is that they give access to the statistics of a number of quite involved 'matter' models of maps equipped with interacting particles or spins. More precisely, we shall focus on the quite general case of Eulerian maps with particles satisfying a nearest-neighbour *p-exclusion rule*. This rule is expressed as follows: each face of the map may be occupied by a number of identical particles with the restriction that there be at most a total of p particles on any pair of adjacent faces [15]. For $p = 1$, the exclusion rule is nothing but the celebrated hard-particle condition that two particles cannot occupy identical nor adjacent sites. In general, in addition to the usual weights g_k and $\tilde{g}_k$ per white and black k-valent face, we attach the weight z_i to each face occupied by i particles (with $z_0 = 1$). All these models are known to undergo various crystallization transitions to ordered phases in which the density of particles on black and on white faces are different (see [15] for details).

The p-exclusion rule may be implemented as follows: we first start by relaxing it and demand only that there be at most p particles on each face. We then introduce on top of any such particle configuration a set of blocked edges on the map, with a weight y per blocked edge, and with the two following restrictions:

(i) as before, we demand that blocked edges satisfy the global connectivity constraint;
(ii) we furthermore restrict the configurations of blocked edges by allowing only for the blocking of those edges which violate the p-exclusion rule for the particle configuration at hand.

As we already know, restriction (i) is crucial to have a mobile description of the configurations at hand. Restriction (ii) is a new constraint but it will be completely transparent in the mobile formalism. Finally, the p-exclusion rule is restored by simply taking $y = -1$ in the various generating functions.

Indeed, note first that whenever the configuration of particles satisfies the p-exclusion rule, we cannot add any blocked edge and it receives the correct weight (irrespectively of the value of y). If the configuration of particles violates the p-exclusion rule, let us show that the contributions of all blocked edge configurations allowed on the map add up to 0. Clearly, if we relax the global connectivity constraint (i), any violated edge can be blocked or not, thus receiving a weight $1 + y = 0$ so that the contribution of all blocked edge configurations vanishes trivially. To prove that the contribution of those configurations that satisfy (i) also vanishes, we therefore need only prove the vanishing of the complementary contribution of those blocked configurations that *do not* satisfy (i). To this end, assume the existence of a maximal connected domain which is not attainable from the origin of the map and consider the boundary of the dual of this domain (see figure 14(*a*)). It consists of a loop of alternating black and white vertices connected via a succession of edges dual to alternatively in- and outgoing edges of the original Eulerian map (see figure 14(*b*)). Clearly, all in-going edges must be blocked to prevent entering the domain. We simply have to show that at least one of the outgoing edges violates the p-exclusion rule so that we may freely decide to block it or not, thus creating a weight $1 + y = 0$ causing the whole contribution to vanish. As all in-going edges are blocked, they violate the exclusion rule; thus, the total number of particles around the loop is larger or equal to $(p + 1)L$ if the loop has length $2L$. Assuming by contradiction that none of the out-going edges violates the exclusion, then the total number of particles around the loop would not exceed pL. This forms a contradiction.

For illustration, we have displayed in figure 15 the allowed blocked edge configurations satisfying (i) and (ii) above for $p = 1$ and for a particular configuration of particles. Their total contribution vanishes when $y = -1$ as the particle configuration at hand violates the 1-particle exclusion rule.

We conclude that the nearest-neighbour interaction of the particle model with p-exclusion rule can be completely undone at the expense of introducing blocked edges on the map. This will allow for a straightforward derivation of recursive equations determining the generating function of the model.

4.2. Generating functions

Let us consider the generating function G of Eulerian maps with particles subject to the p-exclusion rule, with a distinguished origin vertex (pointed maps) and, for convenience, with also a *distinguished edge*. Thanks to the bijection of section 2, G may be expressed in terms of various generating functions for rooted sub-mobiles. More precisely, the mobiles that we have to consider now are unrestricted mobiles supplemented by particles living on their black

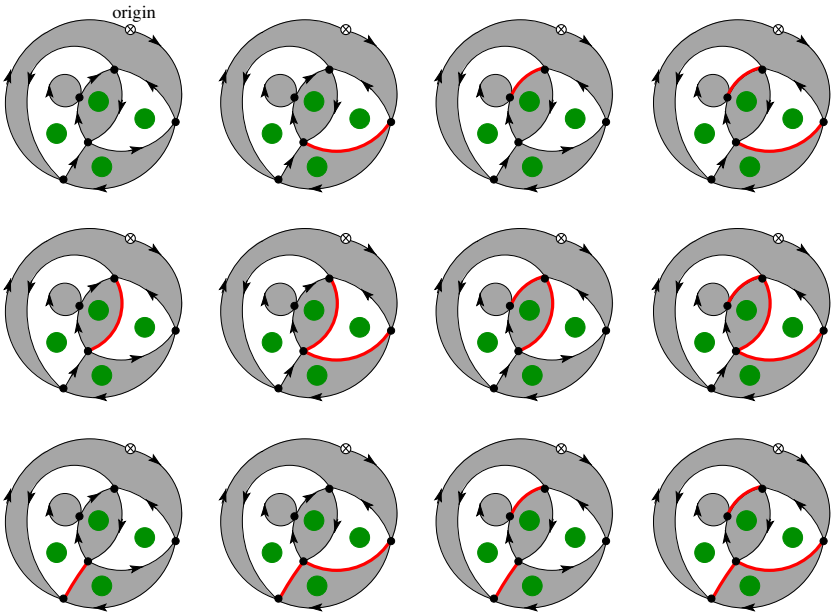

Figure 15. A sample configuration of pointed Eulerian map with four particles (top left) violating the p-exclusion rule, here with $p = 1$. We have listed all possible blocked edge configurations satisfying the global connectivity constraint (i) and the condition (ii) that we may block only edges that violate the 1-exclusion rule. Weighting each blocked edge by $y = -1$, the contributions of the 12 configurations add up to 0, as it should.

and white unlabelled vertices, and with at most p particles per vertex. Given this particle decoration, the only new constraint inherited from the condition (ii) of previous section is that a flagged edge may be marked only if the total number of particles on its two endpoints exceeds p strictly. By a direct generalization of our notations of section 2.4, we may now introduce the following generating functions:

- R denotes as in equation (2.9) the generating function for sub-mobiles rooted at a labelled corner, and with arbitrary (but fixed) root label;
- $B_\ell^{(i)}$ (resp. $\tilde{B}_\ell^{(i)}$) denotes the generating function for sub-mobiles rooted at some un-marked (resp. marked) flagged edge incident to a black vertex carrying i particles and with arbitrary (but fixed) labels on the left and on the right of the edge differing by ℓ (with $\ell \geqslant 0$ in the un-marked case);
- finally, $W_{-\ell}^{(i)}$ (resp $\tilde{W}_{-\ell}^{(i)}$) denotes to the generating function for sub-mobiles rooted at some un-marked (resp. marked) flagged edge incident to a white vertex carrying i particles and with arbitrary (but fixed) labels on the right and on the left of the edge differing by ℓ (with again $\ell \geqslant 0$ in the un-marked case).

By use of a straightforward generalization of equations (2.10) and (2.11) with $y = -1$, the generating function G is now given by

$$G = R + \sum_{i=0}^{p} \sum_{j=0}^{p} \sum_{\ell \geqslant 0} B_\ell^{(i)} W_{-\ell}^{(j)} - \sum_{i=0}^{p} \sum_{j=p+1-i}^{p} \sum_{\ell} \tilde{B}_\ell^{(i)} \tilde{W}_{-\ell}^{(j)}. \tag{4.1}$$

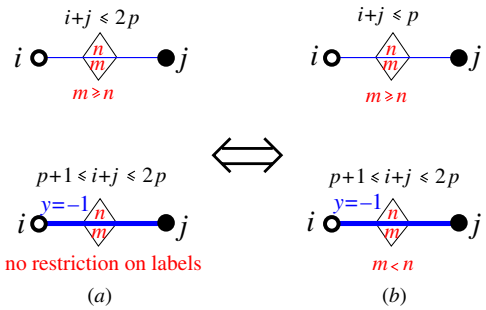

Figure 16. Simplification of the crossing rule when $y = -1$. Here i and j denote the numbers of particles occupying the white and black vertices. The original crossing rule (a) of section 2.2 displayed in figures 4 and 5 can be equivalently replaced by a new crossing rule (b) in which the allowed variation of labels m, n is strictly correlated to the satisfaction ($m \geqslant n$) or violation ($m < n$) of the p-exclusion rule.

Collecting the generating functions of the different sub-mobiles that can be attached to a white (resp. black) vertex carrying i particles, we are led to introduce $p+1$ Laurent series $Q_\circ^{(i)}(z)$ (resp. $Q_\bullet^{(i)}(z)$), $i = 0, \ldots, p$, defined as

$$\begin{aligned} Q_\circ^{(i)}(z) &= \frac{R}{z} + \sum_{j=0}^{p} \sum_{\ell \geqslant 0} B_\ell^{(j)} z^\ell + \sum_{j=p+1-i}^{p} \sum_{\ell} \tilde{B}_\ell^{(j)} z^\ell \\ Q_\bullet^{(i)}(z) &= z + \sum_{j=0}^{p} \sum_{\ell \leqslant 0} W_\ell^{(j)} z^\ell + \sum_{j=p+1-i}^{p} \sum_{\ell} \tilde{W}_\ell^{(j)} z^\ell. \end{aligned} \tag{4.2}$$

All generating functions are now fixed by the recursive relations:

$$\begin{aligned} R &= \frac{1}{1-L}, \qquad L = \sum_k g_k \sum_{i=0}^{p} \left(Q_\circ^{(i)}(z)\right)^{k-1} \big|_{z^1} \\ B_\ell^{(i)} &= z_i \sum_k \tilde{g}_k \left(Q_\bullet^{(i)}(z)\right)^{k-1} \big|_{z^\ell}, \qquad \ell \geqslant 0 \\ \tilde{B}_\ell^{(i)} &= -z_i \sum_k \tilde{g}_k \left(Q_\bullet^{(i)}(z)\right)^{k-1} \big|_{z^\ell} \\ W_\ell^{(i)} &= z_i \sum_k g_k \left(Q_\circ^{(i)}(z)\right)^{k-1} \big|_{z^\ell}, \qquad \ell \leqslant 0 \\ \tilde{W}_\ell^{(i)} &= -z_i \sum_k g_k \left(Q_\circ^{(i)}(z)\right)^{k-1} \big|_{z^\ell}. \end{aligned} \tag{4.3}$$

In particular, note that $\tilde{B}_\ell^{(i)} = -B_\ell^{(i)}$ and $\tilde{W}_{-\ell}^{(i)} = -W_{-\ell}^{(i)}$ for $\ell \geqslant 0$, so that equation (4.1) simplifies into

$$G = R + \sum_{i=0}^{p} \sum_{j=0}^{p-i} \sum_{\ell \geqslant 0} B_\ell^{(i)} W_{-\ell}^{(j)} - \sum_{i=0}^{p} \sum_{j=p+1-i}^{p} \sum_{\ell < 0} \tilde{B}_\ell^{(i)} \tilde{W}_{-\ell}^{(j)} \tag{4.4}$$

while we may write equations (4.2) as

$$\begin{aligned} Q_\circ^{(i)}(z) &= \frac{R}{z} + \sum_{j=0}^{p-i} \sum_{\ell \geqslant 0} B_\ell^{(j)} z^\ell + \sum_{j=p+1-i}^{p} \sum_{\ell<0} \tilde{B}_\ell^{(j)} z^\ell \\ Q_\bullet^{(i)}(z) &= z + \sum_{j=0}^{p-i} \sum_{\ell \leqslant 0} W_\ell^{(j)} z^\ell + \sum_{j=p+1-i}^{p} \sum_{\ell>0} \tilde{W}_\ell^{(j)} z^\ell. \end{aligned} \tag{4.5}$$

In particular, we need only consider generating functions $\tilde{B}_\ell^{(j)}$ for $\ell < 0$ (and $\tilde{W}_\ell^{(j)}$ for $\ell > 0$). This is a direct manifestation of an obvious simplification of the crossing rule for labels on mobiles when $y = -1$, as displayed in figure 16. Any flagged edge whose endpoints have a total number of particles larger or equal to $p + 1$ and with increasing label clockwise around the white endpoint can be marked or not on the mobile, resulting in a weight $1 + y = 0$. The mobiles that survive in practice are therefore mobiles whose flagged edges are of the following two types only (see figure 16(*b*)):

- unmarked flagged edges whose endpoints have a total number of particles smaller or equal to p and with increasing label clockwise around the white endpoint;
- marked flagged edges whose endpoints have a total number of particles larger or equal to $p + 1$ and with strictly decreasing label clockwise around the white endpoint. These edges furthermore receive a weight -1.

As in section 2.4, generalizing (2.14), we may summarize the equations above in a closed system:

$$\boxed{\begin{aligned} Q_\circ^{(i)}(z) &= \frac{R}{z} + \sum_k \tilde{g}_k \sum_{j=0}^{p-i} z_j \left[\left(Q_\bullet^{(j)}(z) \right)^{k-1} \right]_+ - \sum_k \tilde{g}_k \sum_{j=p+1-i}^{p} z_j \left[\left(Q_\bullet^{(j)}(z) \right)^{k-1} \right]_{<0} \\ Q_\bullet^{(i)}(z) &= z + \sum_k g_k \sum_{j=0}^{p-i} z_j \left[\left(Q_\circ^{(j)}(z) \right)^{k-1} \right]_- - \sum_k g_k \sum_{j=p+1-i}^{p} z_j \left[\left(Q_\circ^{(j)}(z) \right)^{k-1} \right]_{>0} \\ R &= 1 + \sum_k g_k \sum_{j=1}^{p} z_j \left[\frac{\left(Q_\circ^{(j)}(z) \right)^{k-1}}{z} \right]_0 R, \end{aligned}} \tag{4.6}$$

where the notations $[\cdot]_{<0}$ and $[\cdot]_{>0}$ stand respectively for the extraction of the negative and positive power parts in the Laurent series of z.

4.3. Detailed study of Eulerian triangulations with hard particles

As an example, let us study in detail the case of Eulerian triangulations with hard-particles, i.e. particles subject to the 1-exclusion rule. This case corresponds to having $g_k = \tilde{g}_k = g\delta_{k,3}$ (as there are as many black and white triangles in an Eulerian triangulations, there is no need to introduce different weight factors for these faces). In a dual formulation, this model is equivalent to that of so-called bicubic maps with hard particles studied in [15] by random matrix techniques and in [14] by combinatorial techniques based on blossom trees. We refer to these references for a description of the physical properties of the model. By a simple look on equations (4.5) and (4.3), we immediately deduce that the only non-vanishing generating functions in this case are $B_2^{(0)}$, $B_\ell^{(1)}$ for $\ell = 2, 5, 8$ and $\tilde{B}_\ell^{(1)}$ for $\ell = -1, -4$ together with their

'white' counterparts $W_{-2}^{(0)}$, $W_{\ell}^{(1)}$ for $\ell = -2, -5, -8$ and $\tilde{W}_{\ell}^{(1)}$ for $\ell = 1, 4$, so that we may write equation (4.5) as

$$\begin{aligned} Q_{\circ}^{(0)}(z) &= \frac{R}{z} + B_2^{(0)} z^2 + B_2^{(1)} z^2 + B_5^{(1)} z^5 + B_8^{(1)} z^8 \\ Q_{\circ}^{(1)}(z) &= \frac{R}{z} + B_2^{(0)} z^2 + \frac{\tilde{B}_{-1}^{(1)}}{z} + \frac{\tilde{B}_{-4}^{(1)}}{z^4} \\ Q_{\bullet}^{(0)}(z) &= z + \frac{W_{-2}^{(0)}}{z^2} + \frac{W_{-2}^{(1)}}{z^2} + \frac{W_{-5}^{(1)}}{z^5} + \frac{W_{-8}^{(1)}}{z^8} \\ Q_{\bullet}^{(1)}(z) &= z + \frac{W_{-2}^{(0)}}{z^2} + \tilde{W}_1^{(1)} z + \tilde{W}_4^{(1)} z^4. \end{aligned} \tag{4.7}$$

Equations (4.3) now translate into

$$\begin{aligned} B_2^{(0)} &= g & W_{-2}^{(0)} &= gR^2 \\ B_2^{(1)} &= gz_1\big((1+\tilde{W}_1^{(1)})^2 + 2W_{-2}^{(0)}\tilde{W}_4^{(1)}\big) & W_{-2}^{(1)} &= gz_1\big((R+\tilde{B}_{-1}^{(1)})^2 + 2B_2^{(0)}\tilde{B}_{-4}^{(1)}\big) \\ \tilde{B}_{-1}^{(1)} &= -2gz_1 W_{-2}^{(0)}\big(1+\tilde{W}_1^{(1)}\big) & \tilde{W}_1^{(1)} &= -2gz_1 B_2^{(0)}\big(R+\tilde{B}_{-1}^{(1)}\big) \\ \tilde{B}_{-4}^{(1)} &= -gz_1\big(W_{-2}^{(0)}\big)^2 & \tilde{W}_4^{(1)} &= -gz_1\big(B_2^{(0)}\big)^2 \end{aligned} \tag{4.8}$$

as well as expressions for $B_5^{(1)}$, $B_8^{(1)}$, $W_{-5}^{(1)}$ and $W_{-8}^{(1)}$ that we shall not use. This allows us to express these generating functions in terms of R only, namely,

$$\begin{aligned} B_2^{(0)} &= g & B_2^{(1)} &= \frac{gz_1\big(1-2g^4z_1R^2-8g^6z_1^2R^3-8g^8z_1^3R^4\big)}{(1+2g^2z_1R)^2} \\ \tilde{B}_{-1}^{(1)} &= -\frac{2g^2z_1R^2}{1+2g^2z_1R} & \tilde{B}_{-4}^{(1)} &= -g^3z_1R^4, \end{aligned} \tag{4.9}$$

while $W_{-2}^{(0)} = R^2B_2^{(0)}$, $W_{-2}^{(1)} = R^2B_2^{(1)}$, $W_1^{(1)} = B_{-1}^{(1)}/R$ and $W_4^{(1)} = B_{-4}^{(1)}/R^4$. Finally, the generating function R itself is given by the recursion relation:

$$\begin{aligned} R &= 1 + gR\big(2R\big(B_2^{(0)} + B_2^{(1)}\big) + 2z_1\big(R + \tilde{B}_{-1}^{(1)}\big)B_2^{(0)}\big) \\ &= 1 + 2g^2R^2\frac{1+2z_1+2g^2(2z_1+z_1^2)R+2g^4z_1^2R^2-8g^6z_1^3R^3-8g^8z_1^4R^4}{(1+2g^2z_1R)^2}. \end{aligned} \tag{4.10}$$

In particular, expanding R in powers of g leads to

$$\begin{aligned} R = 1 &+ 2g^2(1+2z_1) + 4g^4\big(2+8z_1+5z_1^2\big) + 4g^6\big(10+60z_1+89z_1^2+28z_1^3\big) + 32g^8\big(7+56z_1 \\ &+ 135z_1^2+107z_1^3+21z_1^4\big) + 16g^{10}\big(84+840z_1+2828z_1^2+3808z_1^3+1911z_1^4+264z_1^5\big) \\ &+ 64g^{12}\big(132+1584z_1+6870z_1^2+13320z_1^3+11629z_1^4+4088z_1^5+429z_1^6\big) + \mathcal{O}(g^{14}). \end{aligned} \tag{4.11}$$

The desired generating function G for maps can be expressed in terms of R as

$$\begin{aligned} G &= R + B_2^{(0)}W_{-2}^{(0)} + B_2^{(0)}W_{-2}^{(1)} + B_2^{(1)}W_{-2}^{(0)} - \tilde{B}_{-1}^{(1)}\tilde{W}_1^{(1)} - \tilde{B}_{-4}^{(1)}\tilde{W}_4^{(1)} \\ &= R\frac{\big(1+4g^4z_1R^2+g^2(R+6z_1R)-g^6z_1^2R^3-20g^8z_1^3R^4-20g^{10}z_1^4R^5\big)}{(1+2g^2z_1R)^2}. \end{aligned} \tag{4.12}$$

In particular, expanding G in powers of g leads to

$$\begin{aligned} G = 1 &+ 3g^2(1+2z_1) + 12g^4\big(1+4z_1+2z_1^2\big) + 15g^6\big(4+24z_1+33z_1^2+8z_1^3\big) + 48g^8\big(7+56z_1 \\ &+ 130z_1^2+92z_1^3+14z_1^4\big) + 168g^{10}\big(12+120z_1+395z_1^2+500z_1^3+220z_1^4+24z_1^5\big) \\ &+ 144g^{12}\big(88+1056z_1+4512z_1^2+8416z_1^3+6801z_1^4+2080z_1^5+176z_1^6\big) + \mathcal{O}(g^{14}), \end{aligned} \tag{4.13}$$

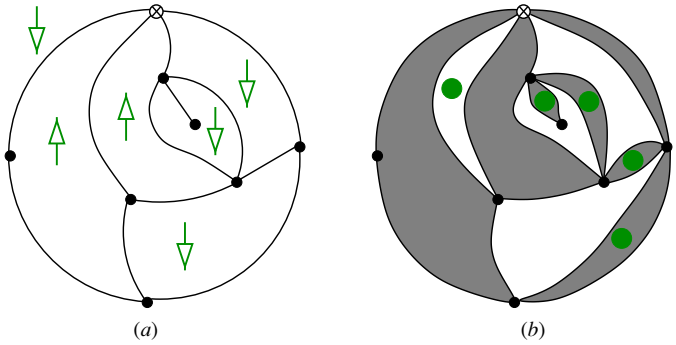

Figure 17. An example (*a*) of quadrangulation with Ising up/down spins on its faces and the equivalent Eulerian map with bi- and tetra-valent black or white faces (*b*). The original spin up (resp. down) faces translate into empty black (resp. white) tetravalent faces, while a bivalent face is introduced between any pair of adjacent faces with equal spins to restore the bicolourability. The same configurations are alternatively selected from all possible Eulerian maps with bi- and tetra-valent faces by adding a particle on each bivalent face and imposing the 1-particle exclusion. This indeed forces the bivalent faces to be isolated and to separate tetravalent faces of identical colour.

which displays the generating functions of Eulerian triangulations with hard particles and with $2, 4, \ldots, 12$ triangles. Note that here, the triangulations have a distinguished origin vertex *and* a distinguished edge. It is more usual to consider so-called rooted maps with a distinguished edge only. As there are $n + 2$ vertices in an Eulerian triangulation with $2n$ faces, this is done here by dividing out the coefficient of g^{2n} by an overall factor $(n + 2)$.

4.4. Ising model revisited

As a final application, let us consider the case of quadrangulations with Ising spins, i.e. maps with tetravalent faces only and with spins up or down living on these faces. The Ising coupling is introduced by a weight, say z_1 per edge separating faces with the same value of the spin, while edges separating faces with opposite spins receive the weight 1 instead. The model may be realized in terms of Eulerian maps with hard-particles as follows (see figure 17): consider Eulerian maps made of

– black or white tetravalent faces that carry no particle;
– black or white bivalent faces that, in contrast, are forced to carry a particle, weighted by z_1.

Assume now that the particles are subject to the 1-particle exclusion rule. This imposes that two bivalent faces cannot be adjacent to one another so that any bivalent face on the map necessarily lies between two tetravalent faces. If the bivalent face is black, the two neighbouring tetravalent faces are necessarily white (and conversely) so that, by squeezing all bivalent faces into single edges, we obtain a quadrangulation with black and white faces and with an effective weight factor z_1 per edge separating two faces of the same colour. This is nothing but the desired Ising model by interpreting the black (resp. white) faces as carrying spins up (resp. down). The Ising model thus corresponds to considering Eulerian maps with particles subject to the 1-particle exclusion rule, with $g_k = \tilde{g}_k = g\delta_{k,4} + z_1\delta_{k,2}$ and with the additional restriction that bivalent faces must carry particles while tetravalent faces must be empty. Again this last restriction is transparent in the mobile formalism as it simply means

that the black and white vertices of the mobile must carry a particle or not according to their valence on the mobile. By a simple look on equations (4.5) and (4.3), we immediately deduce that now, the only non-vanishing generating functions are $B_\ell^{(0)}$ and $B_\ell^{(1)}$ for $\ell = 1, 3$ and $\tilde{B}_\ell^{(1)}$ for $\ell = -1, -3$, together with their white counterparts $W_\ell^{(0)}$ and $W_\ell^{(1)}$ for $\ell = -1, -3$ and $\tilde{W}_\ell^{(1)}$ for $\ell = 1, 3$. We may thus write equation (4.5) as

$$\begin{aligned} Q_\circ^{(0)}(z) &= \frac{R}{z} + B_1^{(0)} z + B_3^{(0)} z^3 + B_1^{(1)} z + B_3^{(1)} z^3 \\ Q_\circ^{(1)}(z) &= \frac{R}{z} + B_1^{(0)} z + B_3^{(0)} z^3 + \frac{\tilde{B}_{-1}^{(1)}}{z} + \frac{\tilde{B}_{-3}^{(1)}}{z^3} \\ Q_\bullet^{(0)}(z) &= z + \frac{W_{-1}^{(0)}}{z} + \frac{W_{-3}^{(0)}}{z^3} + \frac{W_{-1}^{(1)}}{z} + \frac{W_{-3}^{(1)}}{z^3} \\ Q_\bullet^{(1)}(z) &= z + \frac{W_{-1}^{(0)}}{z} + \frac{W_{-3}^{(0)}}{z^3} + \tilde{W}_1^{(1)} z + \tilde{W}_3^{(1)} z^3. \end{aligned} \tag{4.14}$$

Equations (4.3) now translate into

$$\begin{aligned} B_3^{(0)} &= g & W_{-3}^{(0)} &= gR^3 \\ B_1^{(0)} &= 3g\big(W_{-1}^{(0)} + W_{-1}^{(1)}\big) & W_{-1}^{(0)} &= 3gR^2\big(B_1^{(0)} + B_1^{(1)}\big) \\ \tilde{B}_{-3}^{(1)} &= -z_1 W_{-3}^{(0)} & \tilde{W}_3^{(1)} &= -z_1 B_3^{(0)} \\ \tilde{B}_{-1}^{(1)} &= -z_1 W_{-1}^{(0)} & \tilde{W}_1^{(1)} &= -z_1 B_1^{(0)}, \\ B_3^{(1)} &= z_1 \tilde{W}_3^{(1)} & W_{-3}^{(1)} &= z_1 \tilde{B}_{-3}^{(1)}, \\ B_1^{(1)} &= z_1\big(1 + \tilde{W}_1^{(1)}\big) & W_{-1}^{(1)} &= z_1\big(R + \tilde{B}_{-1}^{(1)}\big) \end{aligned} \tag{4.15}$$

from which we deduce all generating functions in terms of R only:

$$\begin{aligned} B_3^{(0)} &= g & B_1^{(0)} &= \frac{3gz_1R}{1 - 3g\big(1 - z_1^2\big)R} \\ B_3^{(1)} &= -gz_1^2 & B_1^{(1)} &= \frac{z_1 - 3gz_1R}{1 - 3g\big(1 - z_1^2\big)R} \\ \tilde{B}_{-3}^{(1)} &= -gz_1R^3 & \tilde{B}_{-1}^{(1)} &= -\frac{3gz_1^2R^2}{1 - 3g\big(1 - z_1^2\big)R} \end{aligned} \tag{4.16}$$

and $W_{-\ell}^{(i)} = R^\ell B_\ell^{(i)}$ for all the values of ℓ and i mentioned above. As for R itself, it now satisfies the recursion relation:

$$\begin{aligned} R &= 1 + R\big(3gR^2\big(B_3^{(0)} + B_3^{(1)}\big) + 3gR\big(B_1^{(0)} + B_1^{(1)}\big)^2 + z_1 B_1^{(0)}\big) \\ &= 1 + 3gR^2 \frac{2z_1^2 - 6g^2R^2\big(1 - z_1^2\big)^2 + 9g^3R^3\big(1 - z_1^2\big)^3 + gR\big(1 - 4z_1^2 + 3z_1^4\big)}{\big(1 - 3g\big(1 - z_1^2\big)R\big)^2}. \end{aligned} \tag{4.17}$$

Note that this equation may be rewritten as

$$\frac{R}{\big(1 - z_1^2\big)} = 1 + 3g^2\big(1 - z_1^2\big)R^3 + \frac{z_1^2}{1 - z_1^2} \frac{R}{\big(1 - 3g\big(1 - z_1^2\big)R\big)^2}, \tag{4.18}$$

which is precisely the form found in [17], [12] and [14]. The first terms of the expansion of R in powers of g read

$$R = 1 + 6gz_1^2 + 3g^2\big(1 + 8z_1^2 + 15z_1^4\big) + 18g^3z_1^2\big(11 + 28z_1^2 + 21z_1^4\big) + 27g^4\big(1 + 31z_1^2$$

$$+229z_1^4+285z_1^6+126z_1^8\big)+54g^5z_1^2\big(97+907z_1^2+2521z_1^4+1929z_1^6+594z_1^8\big)$$
$$+81g^6\big(4+279z_1^2+4833z_1^4+19958z_1^6+30678z_1^8+16419z_1^{10}+3861z_1^{12}\big)+\mathcal{O}(g^7). \tag{4.19}$$

The generating function G for maps is now expressed in terms of R as

$$\begin{aligned} G &= R+B_1^{(0)}W_{-1}^{(0)}+B_3^{(0)}W_{-3}^{(0)}+B_1^{(1)}W_{-1}^{(0)}+B_3^{(1)}W_{-3}^{(0)}+B_1^{(0)}W_{-1}^{(1)}+B_3^{(0)}W_{-3}^{(1)}\\ &\quad -\tilde{B}_{-1}^{(1)}\tilde{W}_1^{(1)}-\tilde{B}_{-3}^{(1)}\tilde{W}_3^{(1)}\\ &= R\frac{1+10g^2R^2\big(1-3z_1^2\big)-6gR\big(1-2z_1^2\big)+9g^4R^4\big(1-z_1^2\big)^2\big(1-3z_1^2\big)-6g^3R^3\big(1-4z_1^2+3z_1^4\big)}{(1-3g(1-z_1)^2R)^2} \end{aligned} \tag{4.20}$$

and expanding $G\equiv G(g,z_1)$ in powers of g leads to

$$\begin{aligned} G(g,z_1) &= 1+12gz_1^2+4g^2\big(1+12z_1^2+18z_1^4\big)+180g^3z_1^2\big(2+5z_1^2+3z_1^4\big)+18g^4\big(2+85z_1^2\\ &\quad +624z_1^4+693z_1^6+252z_1^8\big)+756g^5z_1^2\big(12+119z_1^2+312z_1^4+207z_1^6+54z_1^8\big)\\ &\quad +432g^6\big(1+91z_1^2+1642z_1^4+6681z_1^6+9450z_1^8+4356z_1^{10}+891z_1^{12}\big)+\mathcal{O}(g^7). \end{aligned} \tag{4.21}$$

The coefficient of g^n in G is the generating function of maps with a distinguished origin vertex (among $n+2$) and with a distinguished edge *in the original Eulerian map formulation* with bivalent faces. This means that on the associated quadrangulations, edges separating two faces of the same colour can be marked twice. The number of such edges is given by the power of z_1, so that, in the end, coefficient of $g^n z_1^{2p}$ in (4.21) receives a weight $(n+2)(2n+2p)$ for all possible markings rather than the usual factor $4n$ for rooted quadrangulations with a *distinguished oriented edge* only. We can easily restore this factor and obtain the generating function $H\equiv H(g,z_1)$ for *rooted quadrangulations with Ising spins*, with expansion:

$$\begin{aligned} H(g,z_1) &= 4g\frac{\mathrm{d}}{\mathrm{d}g}\int_0^1\mathrm{d}\alpha\int_0^1\mathrm{d}\beta\frac{\beta}{\alpha}(G(\beta\alpha^2g,\alpha z_1)-1)\\ &= 4gz_1^2+2g^2\big(1+8z_1^2+9z_1^4\big)+108g^3z_1^2\big(1+2z_1^2+z_1^4\big)+12g^4\big(1+34z_1^2\\ &\quad +208z_1^4+198z_1^6+63z_1^8\big)+216g^5z_1^2\big(10+85z_1^2+195z_1^4+115z_1^6+27z_1^8\big)\\ &\quad +54g^6\big(2+156z_1^2+2463z_1^4+8908z_1^6+11340z_1^8+4752z_1^{10}+891z_1^{12}\big)+\mathcal{O}(g^7). \end{aligned} \tag{4.22}$$

5. Conclusion

In this paper, we have considered the combinatorics of the general class of Eulerian maps with blocked edges. This includes a number of matter statistical models on (Eulerian or unrestricted) maps whose local interactions are mediated by the choice of the blocked edge configurations. All these models are amenable to a coding by mobiles, and we obtained the general recursive system of equations that determines the associated generating functions. We gave a number of explicit direct or indirect applications. In particular, this provides a new combinatorial approach to the problem of mutually excluding particles, a set of models that gives access to most relevant RCFT critical points.

The general structure of the recursive equations above involve Laurent series $Q_\bullet(z)$ and $Q_\circ(z)$ or, more generally, operators $\mathbf{Q}_\bullet$ and $\mathbf{Q}_\circ$ which appear as transfer operators describing the evolution of labels around vertices of the mobile. Remarkably, these operator bare a

striking similarity with the 'position' operators standardly introduced in the chain-interacting multimatrix models solved by bi-orthogonal polynomial techniques. In this framework these linear operators correspond to the multiplication by an eigenvalue of some random matrix, usually expressed in the basis of orthogonal polynomials. This similarity was already observed in the simpler mobile or blossom tree descriptions of maps without matter and seems to indicate a deep connection between the existence of bijections with trees and the solvability of the corresponding matrix models via orthogonal polynomials. This is yet to be understood.

At a more practical level, the recursive equations that we face involve in general truncations of the Laurent series $Q_\bullet(z)$ and $Q_\circ(z)$ to *both* their positive and negative parts. In the applications that we discussed, we have explored only particular cases in which either we may get rid of the truncations (section 3) or only a finite number of coefficients in the Laurent series survive (section 4). In the first case, this leads to simple and easily solved algebraic equations for $Q_\bullet(z)$ and $Q_\circ(z)$. In the second case, we end up with a closed algebraic system for the finitely many surviving generating functions. Note that we have not explored the most general case where infinitely many coefficients would survive, as we do not really know how to solve the system of equations in this case. Finding the corresponding solution could give access to more general (non necessarily algebraic) critical behaviours. Such behaviours have been observed for other types of statistical models such as loop models [18], Potts models [19] or the 6-vertex model [20]. The latter correspond to matrix models that were solved by loop equation or saddle point techniques, as no orthogonal polynomial techniques were available. We may wonder whether our general class of Eulerian maps with blocked edges could deal with some of these problems.

To conclude, the general framework of our approach is a modification of the natural notion of geodesic distance on the maps, correlated with the presence of matter. This is a quite natural principle of general relativity, here transposed at a discrete level. In the present construction, the distance was modified by introducing blocked edges but we may imagine other mechanisms. Note finally that our formalism allows in principle to keep track of this modified distance (by keeping track of the labels in generating functions), thus giving access to refined intrinsic geometrical properties of maps with matter.

Acknowledgments

The authors acknowledge support from the Geocomp project, ACI Masse de données, from the ENRAGE European network, MRTN-CT-2004-5616 (PDF and EG) from the ENIGMA European network, MRTN-CT-2004-5652 (PDF) and from the ANR program GIMP, ANR-05-BLAN-0029-01 (PDF).

Appendix A. Combinatorial interpretation of equations (3.7) and (3.10): forests on tetravalent maps as decorated even-valent maps

Equations (3.7) and (3.10) were obtained by use of our mobile formalism but can be given a simple interpretation. These equations are strongly reminiscent of that obeyed by the generating function (still denoted by R) of planar maps with a distinguished face and a distinguished edge and with vertices of arbitrary even valence $2k$, counted with weight v_{2k} (see [9]):

$$R = 1 + \sum_k v_{2k} \binom{2k-1}{k} R^k. \tag{A.1}$$

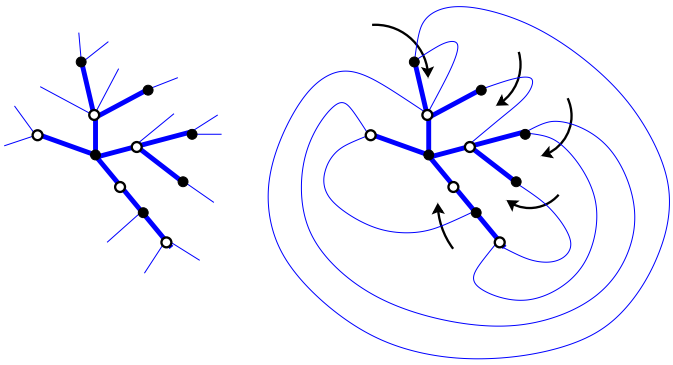

Figure 18. A bicoloured tree with as many black leaves as white leaves (left). There is a unique matching between black and white leaves that can be realized with non-crossing arches and is such that every face can be reached from the external face upon respecting the canonical orientation, i.e. crossing arches with their black endpoint on the right.

Equation (3.10) is recovered by setting

$$v_{2k} = g^{k-1} y^{k-2} \frac{(3k-3)!}{(k-1)!(2k-1)!} \tag{A.2}$$

for all $k \geqslant 2$ and $v_2 = 0$. This relation may be understood as follows: any connected component of the forest with, say $k-1$ tetravalent inner vertices (hence $k-2$ inner edges and $2k$ leaves) can be contracted into a single $2k$-valent vertex by squeezing all its inner edges. Conversely, any $2k$-valent vertex can be expanded into a ternary connected tree with $k-2$ edges in exactly $(3k-3)!/((k-1)!(2k-1)!)$ ways. The enumeration of forests on maps with tetravalent vertices is therefore equivalent to that of maps without forests but with vertices of arbitrary even valences, with the weight factor v_{2k} above simply accounting for the appropriate degeneracy factor in the squeezing process.

Concerning equation (3.7), it differs from equation (3.10) only by an extra factor $(1+y)^{2n}$ which can be simply understood from a 1 to 2^{2n} correspondence, for pointed quadrangulations with $2n$ edges, between allowed configurations of blocked edges where the blockings are necessarily in both directions and allowed configurations of blocked edges where blockings in a single direction are also allowed. The correspondence is as follows: starting from a configuration with edges that are either not blocked or blocked in both directions, we consider for each edge the orientation that leads from its endpoint with a larger distance to the origin to that with a smaller distance (on a quadrangulation, distances between neighbours have different parities so one must be strictly larger than the other). For this particular orientation, we keep the blocked or unblocked nature of the original edge but for the reverse orientation, we decide arbitrarily to block it or not. This leads to 2^{2n} configurations with the *same distance* on the map as the presence or absence of these last blockings clearly does not affect this distance. Collecting the y factors for these 2^{2n} configurations clearly produces a term $(1+y)^{2n}$. The reverse construction is as follows: starting from a configuration with possible blockings in a single direction, we first suppress all blockings oriented from a vertex at smaller distance from the origin to a vertex at larger distance, which leaves us with edges which are either not blocked or blocked in one direction only (one-way edges). We then transform these one-way edges into edges blocked in both directions.

Appendix B. Maximally blocked Eulerian maps

The contribution of Eulerian maps with a maximal number of blocked edges is obtained by taking in equations (2.14) the limit $y \to \infty$ keeping $\alpha_k \equiv g_k y$ and $\tilde{\alpha}_k \equiv \tilde{g}_k y$ finite for all k. In this case, we may write $R = 1 + (1/y)Z + \mathcal{O}(1/y^2)$ where Z is the generating function of maximally blocked Eulerian maps. From equation (2.14), we have the relations

$$\begin{aligned} Z &= \sum_k \alpha_k \left[\frac{Q_\circ^{k-1}(z)}{z} \right]_0 \\ Q_\circ(z) &= \frac{1}{z} + \sum_k \tilde{\alpha}_k Q_\bullet^{k-1}(z) \\ Q_\bullet(z) &= z + \sum_k \alpha_k Q_\circ^{k-1}(z). \end{aligned} \tag{B.1}$$

These equations are recognized as the recursion relations for the generating functions of rooted planar trees whose nodes (inner vertices) have alternating black or white colour, counted with weights α_k per k-valent white node and $\tilde{\alpha}_k$ per k-valent black node. More precisely, interpreting the parameter z as a weight per leaf adjacent to a black node (hereafter referred to as black leaf), while a weight $1/z$ is attached to each leaf adjacent to a white node (white leaf), we see that $(Q_\bullet(z)/z) - 1$ (resp. $zQ_\circ(z) - 1$) is the generating function for such trees with a distinguished white (resp. black) leaf. Rewriting the first line of equation (B.1) as

$$Z = \left[\frac{Q_\bullet(z)}{z} - 1 \right]_0, \tag{B.2}$$

we see that Z can be interpreted as the generating function for *bicoloured trees* with a distinguished white leaf and constrained to have as many white leaves as black leaves. This should not be a surprise. Indeed, in a maximally blocked Eulerian map, the set of edges dual to blocked edges forms a spanning tree of the dual map, which is naturally bicoloured. Each non-blocked edge on the dual map connects nodes of opposite colours: cutting it into two half-edges terminating at leaves results into a bicoloured tree with as many white as black leaves. The original map has a distinguished non-blocked edge, which turns into a distinguish white leaf. Conversely, given a bicoloured tree with as many white leaves as black leaves, there is a *unique* way to connect each black leaf to a white one via non-intersecting arches so that each face of the resulting map can be reached from, say the external face upon respecting the canonical orientation, i.e. crossing edges only with the white endpoint on the left and the black endpoint on the right. This can be done by an iterative matching algorithm: we follow the contour of the tree clockwise and match each black leaf immediately followed by a white leaf to this latter. We then iterate the process by ignoring the already matched leaves until all leaves are matched (see figure 18). The resulting map is clearly dual to a maximally blocked Eulerian map, with a distinguished origin vertex (dual to the external face) and a distinguished non-blocked edge of type $m \to m + 1$ (dual to the edge connecting the distinguished white leaf), and whose blockings satisfy the global connectivity constraint.

References

[1] Tutte W 1962 A Census of planar triangulations *Can. J. Math.* **14** 21–38
Tutte W 1962 A Census of Hamiltonian polygons *Can. J. Math.* **14** 402–17
Tutte W 1962 A Census of slicings *Can. J. Math.* **14** 708–22
Tutte W 1963 A Census of planar maps *Can. J. Math.* **15** 249–71
[2] Kazakov V 1985 Bilocal regularization of models of random surfaces *Phys. Lett.* B **150** 282–4
David F 1985 Planar diagrams, two-dimensional lattice gravity and surface models *Nucl. Phys.* B **257** 45–58

Ambjorn J, Durhuus B and Fröhlich J 1985 Diseases of triangulated random surface models and possible cures *Nucl. Phys.* B **257** 433–49

Kazakov V, Kostov I and Migdal A 1985 Critical properties of randomly triangulated planar random surfaces *Phys. Lett.* B **157** 295–300

[3] Di Francesco P, Ginsparg P and Zinn-Justin J 1995 2D gravity and random matrices *Phys. Rep.* **254** 1–131

[4] Brézin E, Itzykson C, Parisi G and Zuber J-B 1978 Planar Diagrams *Commun. Math. Phys.* **59** 35–51

[5] Cori R and Vauquelin B 1981 Planar maps are well labeled trees *Can. J. Math.* **33** 1023–42

[6] Arquès D 1986 Les hypercartes planaires sont des arbres très bien étiquetés *Discr. Math.* **58** 11–24

[7] Schaeffer G 1997 Bijective census and random generation of Eulerian planar maps *Electron. J. Comb.* **4** R20

See also Schaeffer G 1998 Conjugaison d'arbres et cartes combinatoires aléatoires, *PhD Thesis* Université Bordeaux I

[8] Bousquet-Mélou M and Schaeffer G 2000 Enumeration of planar constellations *Adv. Appl. Math.* **24** 337–68

[9] Bouttier J, Di Francesco P and Guitter E 2002 Census of planar maps: from the one-matrix model solution to a combinatorial proof *Nucl. Phys.* B **645** [PM] 477–99 (*Preprint* cond-mat/0207682)

[10] Chassaing P and Schaeffer G 2004 Random planar lattices and integrated SuperBrownian excursion *Probab. Theory Relat. Fields* **128** 161–212 (*Preprint* math.CO/0205226)

[11] Bouttier J, Di Francesco P and Guitter E 2004 Planar maps as labeled mobiles *Elec. J. Comb.* **11** R69 (*Preprint* math.CO/0405099)

[12] Bousquet-Mélou M and Schaeffer G 2002 The degree distribution in bipartite planar maps: application to the Ising model *Preprint* math.CO/0211070

[13] Bouttier J, Di Francesco P and Guitter E 2003 Combinatorics of hard particles on planar graphs *Nucl. Phys.* B **655** 313–41 (*Preprint* cond-mat/0211168)

[14] Bouttier J, Di Francesco P and Guitter E 2005 Combinatorics of bicubic maps with hard particles *J. Phys. A: Math. Gen.* **38** 4529–60 (*Preprint* math.CO/0501344)

[15] Bouttier J, Di Francesco P and Guitter E 2002 Critical and tricritical hard objects on bicolorable random lattices: exact solutions *J. Phys. A: Math. Gen.* **35** 3821–54 (*Preprint* cond-mat/0201213)

[16] Duplantier B and Kostov I K 1988 Conformal spectra of polymers on a random surface *Phys. Rev. Lett.* **61** 1433–7

Duplantier B and Kostov I K 1990 Geometrical critical phenomena on a random surface on arbitrary genus *Nucl. Phys.* B **340** 491–541

[17] Boulatov D and Kazakov V 1987 The Ising model on a random planar lattice: the structure of the phase transition and the exact critical exponents *Phys. Lett.* B **186** 379–84

[18] Kostov I K 1989 $O(n)$ vector model on a planar random lattice: spectrum of anomalous dimensions *Mod. Phys. Lett.* A **4** 217–26

Eynard B and Zinn-Justin J 1992 The $O(n)$ model on a random surface: critical points and large order behaviour *Nucl. Phys.* B **386** 558–91 (*Preprint* hep-th/9204082)

Eynard B and Kristjansen C 1995 Exact solution of the $O(n)$ model on a random lattice *Nucl. Phys.* B **455** 577–618 (*Preprint* hep-th/9506193)

[19] Daul J M 1995 Q-states Potts model on a random planar lattice *Preprint* hep-th/9502014

Bonnet G and Eynard B 1999 The Potts-q random matrix model: loop equations, critical exponents, and rational case *Phys. Lett.* B **463** 273–9 (*Preprint* hep-th/9906130)

[20] Kazakov V and Zinn-Justin P 1999 Two-matrix model with ABAB interaction *Nucl. Phys.* B **546** 647–68 (*Preprint* hep-th/9808043)

Kostov I K 2000 Exact solution of the six-vertex model on a random lattice *Nucl. Phys.* B **575** 513–34 (*Preprint* hep-th/9911023)